Supercontinuum Generation in a Silicon Nanowire Embedded Photonic Crystal Fiber

E. Gunasundari[1], **Abdosllam M. Abobaker**[2], **K. Senthilnathan**[1], **S. Sivabalan**[3], **K. Nakkeeran**[4], **and P. Ramesh Babu**[1]

[1]Photonics, Nuclear and Medical Physics Division
School of Advanced Sciences, VIT University, Vellore 632 014, India
[2]Department of Communications Engineering, College of Electronic Technology, Bani Walid, Libya
[3]School of Electrical Engineering, VIT University, Vellore 632 014, India
[4]School of Engineering, University of Aberdeen, Aberdeen AB24 3UE, UK

Abstract— In this paper, we demonstrate the supercontinuum generation in a silicon nanowire embedded photonic crystal fiber (SN-PCF) using fully-vectorial finite element method. The variation of supercontinuum is investigated by changing the fiber length, pump peak power and pump wavelength. The proposed fiber exhibits broad spectrum of more than 2200 nm within 2 mm length of fiber for peak power of 500 W of input pulse.

1. INTRODUCTION

The photonic crystal fiber (PCF) is a good platform for manipulating tunable dispersion with high nonlinear properties by arranging the air-holes in the core-cladding geometry suitably. PCF has been an intense topic of research for supercontinuum generation (SCG) ever since the work by Ranka et al [1, 2]. Pumping near a zero dispersion wavelength (ZDW) with high nonlinearity facilitates less power requirement. SCG finds wide applications in different fields such as wavelength division multiplexing [3, 4], optical sensing [5], spectroscopy [6, 7], optical coherence tomography (OCT), etc..

There have been many theoretical and experimental reports of SCG in various guided-wave structures, such as single-mode fibers, PCF, silica nanowires, etc.. The previous results suggest that it is possible to achieve SCG at low optical power and over short propagation distances provided the guiding medium exhibits high nonlinear response and tunable dispersion properties. In a typical PCF based supercontinuum source, the effective mode area of the PCF is roughly $\sim 1\,\mu\text{m}^2$ with several metres of PCF. Further, by reducing the core down to nm size and by tapering the micro-structured core, the effective optical nonlinearity can be increased [8]. Although these previous studies have demonstrated efficient generation of supercontinuum in on-chip integration, those sources demand a large propagation length for generating high spectral broadening.

A promising alternative solution is provided by silicon waveguide sources [9], which have the advantage of employing an emerging silicon-on-insulator (SOI) integrated-photonics platform. Silicon has excellent transmission properties compared to silica and does not require high power density to bring in nonlinearity owing to its huge nonlinear coefficient. Till date, many reports for SCG in silicon nanowire are available [8, 10, 11]. Recently, the possibility of SCG of 500 nm bandwidth at telecommunication wavelength has been demonstrated with various input peak powers for various SOI waveguide lengths. Such a dielectric silicon waveguide with a nanocore diameter could provide a remarkably strong field confinement, enhanced light-matter interactions and strong tunable dispersions when embedded into PCF. The resulting silicon photonic device known as silicon nanowire embedded photonic crystal fiber (SN-PCF) has been proposed very recently [12]. In this paper, we report the supercontinuum of bandwidth wider than 500 nm in SN-PCF with less input peak power.

The paper is laid out as follows. In Section 2, we discuss the design of a SN-PCF using a fully-vectorial finite element method. We study the optical properties of SN-PCF including group velocity dispersion (GVD), third order dispersion (TOD) and nonlinearity by varying the core diameter in Section 3. We investigate the evolution of supercontinuum by changing the fiber length, pump peak power and pump wavelength for 480 nm core diameter in Section 4. Finally, we summarize the findings in Section 5.

2. DESIGN OF THE PROPOSED SN-PCF

The schematic cross section and mode field distribution at $0.8\,\mu\text{m}$ wavelength for 480 nm core diameter of the proposed SN-PCF as shown in Figs. 1(a) and (b). It is composed of circular air holes in the cladding arranged in a triangular pattern and a circular nanosize core. Here, the air-hole diameter is 1120 nm. We analyze the optical properties by increasing the core diameter from 420 to 480 nm. We have already explored all the optical properties for the various core diameters ranging from 1000 to 300 nm [12]. In this work, we choose to vary the core diameter from 420 to 480 nm for analyzing the optical properties for a wavelength range from 0.8 to 1.7 μm for supercontinuum generation. The justification for this range of study is because of tight mode confinement within the core and nearly zero dispersion with high nonlinearity. In order to determine the dispersion of SN-PCF, it is necessary to compute the effective refractive index of the fundamental mode and the same is done by finite element method.

3. OPTICAL PROPERTIES

In this section, we explore the various linear and nonlinear optical properties. We study the impact of dispersions of fundamental mode for different core diameters. The variations of GVD and TOD with respect to wavelength for various core diameters are shown in Fig. 2(a). As is seen in Fig. 2(a), when the core diameter is reduced from 480 nm to 440 nm, the GVD decreases upon increasing the wavelength due to the increase in field distribution towards the core-cladding boundary. However, at 420 nm core diameter, the GVD decreases up to 1.65 μm wavelength beyond which, this dispersion switches to normal regime. From the Fig. 2(a), it is clear that the 480 nm core diameter exhibits a less anomalous GVD ($-0.4909\,\mathrm{ps}^2/\mathrm{m}$) at 0.8 μm wavelength. Further, we report a less TOD ($0.6595 \times 10^{-3}\,\mathrm{ps}^3/\mathrm{m}$) at 0.8 μm wavelength for 480 nm core diameter and this is evident from Fig. 2(a).

Due to the small core diameter and high nonlinear index coefficient of silicon ($4 \times 10^{-18}\,\mathrm{m}^2/\mathrm{W}$), the SN-PCF exhibits tight mode confinement compared to conventional PCF. But a significant fraction of the optical mode propagates in air as the evanescent field. Hence, an accurate estimation

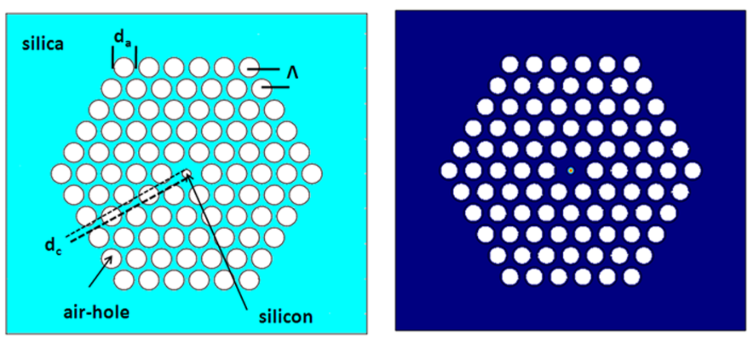

(a) (b)

Figure 1: (a) Geometrical structure of the proposed fiber and (b) mode field distribution at 0.8 μm wavelength for 480 nm core diameter.

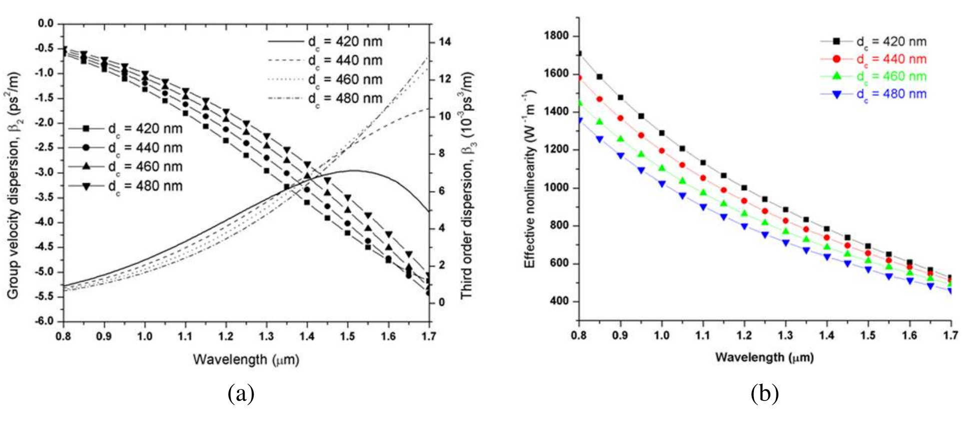

(a) (b)

Figure 2: (a) Variations of GVD and TOD and (b) variations of nonlinearity of the proposed SN-PCF for different core diameters.

of the nonlinear coefficient γ^V is needed for small core diameter. It is known that the mode confinement determined by the effective mode area becomes much pronounced upon reducing the core diameter of the proposed fiber. Fig. 2(b) depicts the variation of effective nonlinearity with respect to wavelength for various core diameters. The results show a slowly decreasing nonlinearity with the increase in wavelength. The proposed structure possesses a maximum effective nonlinearity for lower wavelengths at 420 nm core diameter.

4. SIMULATION OF SUPERCONTINUUM GENERATION

We study the SCG using the generalized nonlinear Schrödinger equation with the effects of two photon absorbtion and free-carrier absorbtion using the proposed SN-PCF as follows [10],

$$\frac{\partial A}{\partial z} = -\frac{1}{2}(\alpha + \alpha^f)A - \frac{i}{2}\beta_2\frac{\partial^2 A}{\partial T^2} + \frac{\beta_3}{6}\frac{\partial^3 A}{\partial T^3} + i\gamma^V\left[1 + \omega/\omega_0\right]A\int_{-\infty}^{\infty}\left[R(T-\tau)|A|^2\right]d\tau \tag{1}$$

where, $A(z,T)$, α, α^f, β_2, β_3, γ^V and $R(T-\tau)$ represent the field envelope, linear loss, free-carrier contribution term, GVD, TOD, effective nonlinearity and Raman response function. In this simulation, we ignore the effects of free carrier absorption, two photon absorption and loss owing to their insignificant role in the interaction. The nonlinear response function $R(t)$ is defined by [10] $R(t) = \gamma(1 - f_R)\delta(t) + f_R h_R(t)$, includes both instantaneous electronic and delayed Raman contributions. The fractional Raman contribution is $f_R = 0.043$ and delayed Raman response $h_R(t)$ of silicon is expressed as: $h_R(t) = \Omega_R^2\tau_1\exp(\frac{-T}{\tau_2})\sin(\frac{T}{\tau_1})$, where the parameters τ_1 ($= 10$ fs) and τ_2 ($= 3$ ps) correspond to the Raman shift and the bandwidth of the Raman gain spectrum,

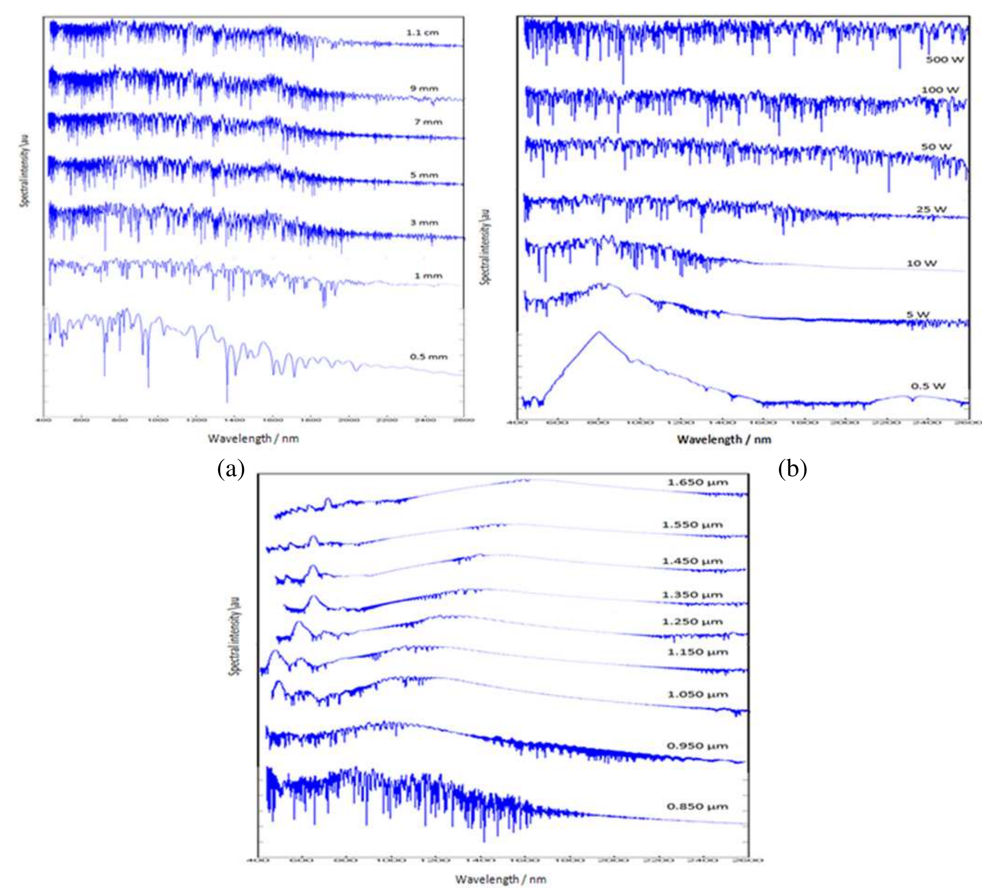

(a) (b)

(c)

Figure 3: Measured supercontinua in the SN-PCF with (a) the different fiber lengths at the pump wavelength of 0.8 µm for the input peak power of 25 W and pulse duration of 50 fs, (b) the pump peak power increasing from 0.5 W to 500 W at the pump wavelength of 0.8 µm of 2 mm of SN-PCF and (c) different pump wavelengths from 0.850 µm to 1.650 µm for the input peak power of 25 W and width of the pulse is 50 fs.

respectively. We investigate the pulse propagation in SN-PCF by symmetrized split-step Fourier method [13]. We consider the input electric field with an input soliton order (N) is given by [14], $A(0,t) = N\sqrt{P_0} sech[\frac{t}{T_0}]$, where P_0 is the peak power and T_0 is the input soliton duration defined as $T_{FWHM}/1.763$, where T_{FWHM} is the full width at half maximum (FWHM) of the input pulse. The soliton order of the input pulse is determined by both pulse and fiber parameters through $N^2 = \frac{L_D}{L_{NL}}$. Here, $L_D = \frac{T_0^2}{|\beta_2|}$ and $L_{NL} = \frac{1}{\gamma P_0}$ are the characteristic dispersive and nonlinear length scales, respectively.

5. RESULTS AND DISCUSSIONS

In this section, first, we investigate the evolution of supercontinuum by varying the length of the fiber using hyperbolic secant input pulse with pulse width of 50 fs. When pumping the pulse in the anomalous dispersion regime nearest to ZDW, the wider spectrum occurs due to the cumulative effect of dispersive waves, soliton fission and Raman soliton self-frequency shift. The spectra of supercontinuum in the SN-PCF with different length of fibers, i.e., $L = 0.5, 1, 3, 5, 7, 9$, and 11 mm for a less input peak power of 25 W are shown in Fig. 3(a).

Second, we study the supercontinuum evolutions by increasing the pump peak power from 0.5 to 500 W at 0.8 μm wavelength in an SN-PCF of 2 mm length as shown in Fig. 3(a). We note that L_D is much larger than L_{NL} when peak power is 0.5 W. At this juncture, SCG is initiated by the self-phase modulation (SPM) and the same is shown in Fig. 3(b). When the pump peak power further increases, the spectrum is broadened by the combined action of SPM, soliton fission and Raman effect. As a result, we obtain a broad spectrum of 1530 nm for a range of wavelengths from 420 to 1950 nm as shown in Fig. 3(b). Thus, the proposed SN-PCF exhibits a narrow spectrum of 300 nm when peak power is relatively less (0.5 W). On the other hand, a wider spectrum of 2100 nm is observed for a maximum peak power of 500 W.

Finally, we investigate the variations of supercontinuum for an input peak power of 25 W with 50 fs pulse width by varying the pump wavelengths from 0.850 to 1.650 μm in a 2 mm length of SN-PCF as shown in Fig. 3(c). We obtain a broad spectrum at shorter wavelength of 0.850 μm due to the effects of low anomalous GVD with high nonlinearity. Further, upon increasing the pump wavelength, we observe a narrow spectrum as order of the soliton is less.

6. CONCLUSION

We have demonstrated the supercontinuum using a silicon nanowire embedded photonic crystal fiber. Further, we have investigated the supercontinuum by varying the length of the fiber, peak power of the input pulse and operating wavelength. We have observed a wider bandwidth exceeding 1300 nm in a 11 mm length of SN-PCF. Further, we have obtained a broad spectrum of more than 2200 nm for a large input peak power of 500 W. Finally, we have obtained a broad spectrum exceeding 1500 nm at a shorter wavelength of 0.850 μm.

ACKNOWLEDGMENT

KSN wishes to thank CSIR [No. 03(1264)/12/EMR-II] and DST [No. SR/FTP/PS-66/2009], Government of India, for the financial support through the sponsored projects. SS wishes to thank DST [No. SR/S2/LOP-0014/2012], Government of India, for the financial support through the sponsored project.

REFERENCES

1. Ranka, J. K., R. S. Windeler, and A. J. Stentz, "Visible continuum generation in air silica microstructure optical fibers with anomalous dispersion at 800 nm," *Opt. Lett*, Vol. 25, No. 1, 25–27, 2000.
2. Liao, M., X. Yan, G. Qin, C. Chaudhari, T. Suzuki, and Y. Ohishi, "A highly non-linear tellurite microstructure fiber with multi-ring holes for supercontinuum generation," *Opt. Express*, Vol. 17, No. 18, 15481–15490, 2009.
3. Morioka, T., H. Takara, S. Kawanishi, O. Kamatani, K. Takiguchi, K. Uchiyama, M. Saruwatari, H. Takahashi, M. Yamada, T. Kanamori, and H. Ono, "1 Tbit/s (100 Gbit/s10 channel) OTDM/WDM transmission using a single supercontinuum WDM source," *Electron. Lett.*, Vol. 32, No. 10, 906–907, 1996.

4. Nakasyotani, T., H. Toda, T. Kuri, and K. Kitayama, "Wavelength-division-multiplexed millimeter-waveband radio-on-fiber system using a supercontinuum light source," *J. Lightwave Technol.*, Vol. 24, No. 1, 404–410, 2006.
5. Kaminski, C. F., R. S. Watt, A. D. Elder, J. H. Frank, and J. Hult, "Supercontinuum radiation for applications in chemical sensing and microscopy," *Appl. Phys. B*, Vol. 92, 367–378, 2008.
6. Liu, Y., M. D. King, H. Tu, Y. Zhao, and S. A. Boppart, "Broadband nonlinear vibrational spectroscopy by shaping a coherent fiber supercontinuum," *Opt. Express*, Vol. 21, No. 7, 8269–8275, 2013.
7. Sanders, S. T., "Wavelength-agile fiber laser using group-velocity dispersion of pulsed super-continua and application to broadband absorption spectroscopy," *Appl. Phys. B*, Vol. 75, No. 7, 799–802, 2002.
8. Foster, M., A. L. Gaeta, Q. Cao, and R. Trebino, "Soliton-effect compression of supercontinuum to few-cycle durations in photonic nanowires," *Opt. Express*, Vol. 13, No. 18, 6848–6855, 2005.
9. Boyraz, Ö., P. Koonath, V. Raghunathan, and B. Jalali, "All optical switching and continuum generation insilicon waveguides," *Opt. Express*, Vol. 12, No. 17, 4094–4102, 2004.
10. Yin, L., Q. Lin, and G. P. Agrawal, "Soliton fission and supercontinuum generation in silicon waveguides," *Opt. Lett.*, Vol. 32, No. 4, 391–393, 2007.
11. Driscoll, J. B., X. Liu, S. Yasseri, I. Hsieh, J. I. Dadap, and R. M. Jr. Osgood, "Large longitudinal electric fields (E_z) in silicon nanowire waveguides," *Opt. Exp.*, Vol. 17, No. 4, 2797–2804, 2009.
12. Gunasundari, E., K. Senthilnathan, S. Sivabalan, M. Abdosllam Abobaker, K. Nakkeeran, and P. Ramesh Babu, "Waveguiding properties of silicon nanowire embedded photonic crystal fiber," *Opt. Materials*, Vol. 36, No. 5, 958–964, 2014.
13. Dudley, J. M. and J. R. Taylor, *Supercontinuum Generation in Optical Fibers*, Cambride University Press, 2010.
14. Agrawal, G. P., *Nonlinear Fiber Optics*, Academic Press, 2007.